IEEE Access
Multidisciplinary | Rapid Review | Open Access Journal

Received July 12, 2019, accepted August 1, 2019, date of publication August 6, 2019, date of current version August 22, 2019.

Digital Object Identifier 10.1109/ACCESS.2019.2933447

Robust DOBC for Stabilization Loop of a Two-Axes Gimbal System

WEI REN, QI QIAO, KANG NIE, AND YAO MAO, (Member, IEEE)
Institute of Optics and Electronics, Chinese Academy of Sciences, Chengdu 610209, China
Key Laboratory of Beam Control, Chinese Academy of Sciences, Chengdu 610209, China
University of Chinese Academy of Sciences, Beijing 100039, China

Corresponding author: Yao Mao (maoyao@ioe.ac.cn)

ABSTRACT In this paper, a disturbance compensation strategy based on disturbance observer control (DOBC) is proposed to solve parameter perturbation, friction, coupling and external turbulence for two-axes gimbal control system. Uncertainties, friction, coupling shortcoming of gimbal system is summed up as a disturbance suppression problem, and achieving disturbance compensation through feedforward channel of DOBC. However, the compensation effects of DOBC are determined by modeling accuracy of the nominal plant and feedforward filter design. A $H\infty$-based filter design is adopted to guarantee robust stability of DOBC when controlled object changed. Because performance weight function of DOBC is derived from stable constraint of closed-loop system, and robust of closed-loop system can also be satisfied. Eventually, we completed proof of $H\infty$-based robust DOBC algorithm in pod system, and stability performance of the system has been greatly improved.

INDEX TERMS Disturbance observe control, disturbance suppression, robust stability, $H\infty$.

I. INTRODUCTION

In the field of target measuring, laser or quantum communication, target tracking, two-axes gimbal system with azimuth-axis and elevation-axis is widely applied because of the broad operation range in space area [1]–[5]. In order to isolate disturbances from base and environment, the gyros are selected as a feedback sensor of inertial velocity of gimbal to inhibit external disturbance torque and make sure inertial stability of the system. Its ultimate goal is to provide adequate stability for outer position tracking loop. However, gimbal system encounters not only external turbulence but also effects of friction characteristic and coupling between two axes. Dynamic characteristic of gimbal system must be affected as a result of friction and coupling no matter what working conditions. Especially, friction belongs to a nonlinear disturbance which is difficult to portray by mathematical modeling. But in moving platform, the most perturbation problem of gimbal system is disturbance torque caused by external vibration.

For the disturbance suppression researches of gimbal system, [6]–[8] utilize $H\infty$-norm robust design method respectively to achieve robust velocity controller of the line-of-sight (LOS) system. In order to compensate friction effects, Bo Li proposed a simple linear quadratic Gaussian algorithm, which can estimate friction disturbance online [9]. In [10], the authors combined time-delay estimation method with two-degree-of-freedom (2-DOF) internal model control to validly compensate nonlinear friction. Recently, a series of advanced control strategies are successfully applied in the gimbal system by some academicians. [11] used extend state observer of ADRC to observe and reject external disturbance and internal parameter perturbation. Literature [12] shows a self-tuning PID type fuzzy controller design method which compares with traditional PI controller, which has even less response time and smaller overshooting, to ensure better applicability in different work conditions. An adaptive fractional-order sliding-mode method can be compensated adaptively according to the change of disturbance torque that is proposed, and the stability of the closed-loop system is proved based on Lyapunov function [13]. These research methods have achieved compensation and suppression of disturbance of the gimbal system to a certain extent.

From the disturbance estimation and compensation point of view, we introduce DOBC into velocity stabilization loop

The associate editor coordinating the review of this manuscript and approving it for publication was Azwirman Gusrialdi.

of gimbal system in order to improve the system disturbance rejection ratio in this paper. The DOBC structure was proposed by Ohnishi in 1987 [14] and has been widely used in motion control. The main idea of DOBC is to estimate disturbance signals depending on its nominal model, then feedforward to the closed-loop through filter to offset the effects of disturbance. Three conflicting performances have been, how to better balance disturbance rejection, noise suppression and robust stability in the DOBC design process, the focus of research [15]–[18]. The author of [19] analyzed in detail the influence of the numerator order, denominator order, and time constant of the DOBC filter on the disturbance suppression, robust performance and noise suppression in the second-order system, which gives corresponding design guidance. [20] also presented a sensitivity optimization approach for the design of DOBC. However, there are various nonlinear disturbances, dynamic characteristics changes and modeling errors in the system, and the traditional DOBC design algorithm based on the nominal model lacks rigorous robust theoretical analysis of the system. Further, [21] proposed a graphical DOBC design method using frequency response analysis. In [22], [23], DOBC filter design under the performance constraints is implemented by the $H\infty$ method. Moreover, an extended $H\infty$ control based on disturbance observation is proposed [24]. These methods analysis and give the robust stability constraints based on the uncertainty of the system, and eventually realize the robust design of DOBC.

In this paper, we consider the amount of disturbance observed in the DOBC structure as the sum of external disturbances, internal frictional disturbances, coupling moments, and modeling errors faced by the gimbal system. Compared with traditional PID closed-loop control, it is reasonable to believe that a gimbal control system with a DOBC compensation structure will exhibit better disturbance suppression performance. However, the perturbation of the gimbal object model can cause the DOBC to compromise the stability of the closed loop system. Therefore, based on the previous theory, this paper further designs a $H\infty$ norm to solve problem of Q filter from the frequency domain perspective, and realizes a simpler solution method by using the performance index of the pre-implemented stable closed-loop system.

This paper is organized as follows. Section 2 analyses kinetic relationship of two-axes gimbal and formulates the disturbing problem of gimbal. In section 3, a design method of DOBC filter based on $H\infty$ is discussed in detail. The proposed robust DOBC design procedure is applied to the pod system, and the experiment results are presented in Section 4. Finally, conclusions are given in Section 5.

II. MODELING ANALYSIS OF TWO-AXES GIMBAL SYSTEM

Two-axes gimbal system can be described by azimuth-axis frame A, elevation-axis frame E and a frame B fixed to fuselage body, respectively (Figure 1). The gyro sensors are placed on the azimuth and elevation axes to measure velocity signal of the corresponding rotation shaft. The velocity

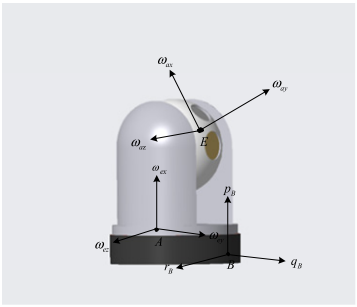

FIGURE 1. Two-axes gimbal system.

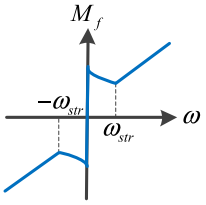

FIGURE 2. LuGre friction model.

stabilization closed-loop control of the two-axes is completed based on the velocity feedback signal, and the stability of the two axes in the inertial space and the precise follow-up of the specified velocity input are realized. Finally, the stability and pointing precision of the pointing axis are ensured.

The angular velocity vector of frame A, E, and B can be respectively expressed as

$$\omega_A = [\omega_{ax} \quad \omega_{ay} \quad \omega_{az}]^T \tag{1}$$

$$\omega_E = [\omega_{ex} \quad \omega_{ey} \quad \omega_{ez}]^T \tag{2}$$

$$\omega_B = [p_B \quad q_B \quad r_B]^T \tag{3}$$

The three axes components of every frames are denoted by roll, yaw and elevation. Assume that the coordinate center points of the three frames are the same point. When the rotation angle of A with respect to B is φ and E is rotated by θ with respect to A, according to Euler's theorem, the corresponding transformation matrices is obtained

$$R_{A,\varphi} = \begin{bmatrix} \cos\varphi & \sin\varphi & 0 \\ -\sin\varphi & \cos\varphi & 0 \\ 0 & 0 & 0 \end{bmatrix} \tag{4}$$

$$R_{E,\theta} = \begin{bmatrix} \cos\theta & 0 & -\sin\theta \\ 0 & 1 & 0 \\ \sin\theta & 0 & \cos\theta \end{bmatrix} \tag{5}$$

The inertia matrices of azimuth and elevation gimbals are

$$\text{Azimuth axis: } J_A = \begin{bmatrix} J_{ax} & D_{xy} & D_{xz} \\ D_{xy} & J_{ay} & D_{yz} \\ D_{xz} & D_{yz} & J_{az} \end{bmatrix} \tag{6}$$

$$\text{Elevation axis: } J_E = \begin{bmatrix} J_{ex} & K_{xy} & K_{xz} \\ K_{xy} & J_{ey} & K_{yz} \\ K_{xz} & K_{yz} & J_{ez} \end{bmatrix} \tag{7}$$

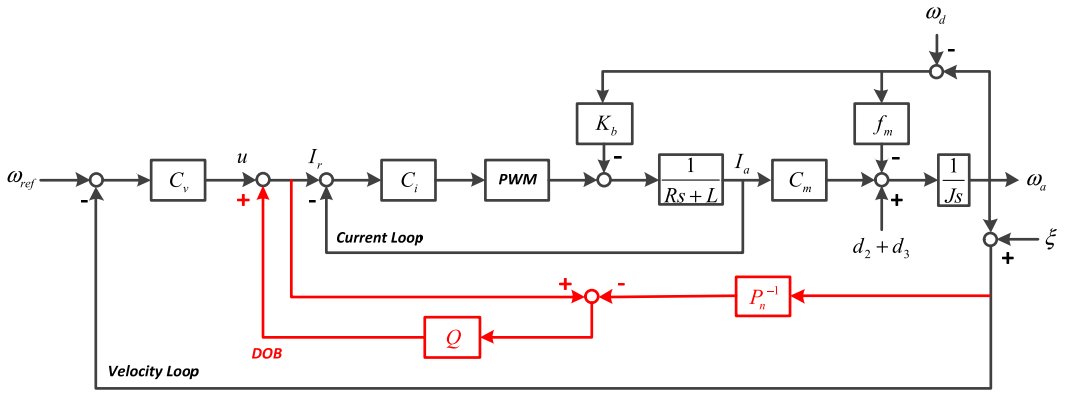

FIGURE 3. The control structure of two-axes gimbal system based on DOBC.

D and K are the inertial coupling coefficients between the axes, respectively. According to the Euler rotation angle relationship and the rotational inertia relationship matrix, the total torque T acting on each axis of the frame can be described as

$$T = \frac{d}{dt}\bar{H} + \bar{\omega} \times \bar{H} \tag{8}$$

In which the angular momentum is defined by $\bar{H} = J\bar{\omega}$. $\bar{\omega}$ expresses the body inertial rate in the body fixed frame, and J is the body inertia matrix.

Further, the motion equation of gimbal is obtained as follows

$$J\dot{\bar{\omega}} = T_m + T_d \tag{9}$$

where T_m is the controlling torque of motor, T_d depicts a total disturbance torque include friction torque d_1, coupling torque d_2 and external disturbance torque d_3.

$$T_d = d_1 + d_2 + d_3 \tag{10}$$

d_1 is the total friction disturbance of the gimbal, which is comprised by the maximum static friction, coulomb friction, and viscous friction. Concretely, the LuGre model can be used to describe the relationship between the angular velocity ω and the friction torque M_f:

$$M_f = M_c + (M_m - M_c)e^{-(\frac{\omega}{\omega_{str}})^2} + f_m\omega \tag{11}$$

where M_m is the maximum static friction torque, M_c is the Coulomb friction, f_m is the viscous friction, and ω_{str} represents stribeck characteristic velocity. The maximum static friction torque is greater than the Coulomb friction torque, and the Coulomb friction torque is constant during the rotation. Due to the effects of these nonlinear friction, gimbal system will have low-speed crawling problem. Moreover, actual friction model is varied when gimbal is in the different directions of rotation.

The effects of external physical disturbance torque such as wind disturbance and carrier vibration on the gimbal are defined as d_2. d_3 represents the coupling relationship between the azimuth-axis and elevation-axis, which generate mutual coupling moments during the movement of the frame.

The azimuth-axis and elevation-axis of the gimbal are respectively subjected to the coupling torque T_a and T_e

$$\begin{aligned} T_a = {} & (D_{xy}\sin\varphi - D_{yz}\cos\varphi)\dot{\omega}_{ey} \\ & + (D_{xy}\cos\varphi + D_{yz}\sin\varphi)\omega_{ey}^2 \\ & + [(J_{az} - J_{ax})\sin(2\varphi) + 2D_{xz}\cos(2\varphi)]\omega_{ey}\omega_{az} \end{aligned} \tag{12}$$

$$\begin{aligned} T_e = {} & (D_{xy}\sin\theta - D_{yz}\cos\theta)\dot{\omega}_{az} \\ & - 0.5[(J_{ez} - J_{ex})\sin 2\theta + 2D_{xz}\cos 2\theta]\omega_{az}^2 \end{aligned} \tag{13}$$

Under the influence of various nonlinear disturbances and couplings, the model characteristics of the gimbal have a certain degree of parameters perturbation. The closed-loop control based on PID and zero-pole cancellation can guarantee the robust stability of the system. However, disturbance suppression performance expected in the system design cannot be achieved.

Generally, the control structure of the gimbal consists of a current loop and a velocity loop, as shown in Figure 3. The current loop is used to overcome the influence of the inductance value waves of the reactor, improving the dynamic response capability of the current. Further the characteristics of controlled object of velocity stability loop is improved, and the influence of current fluctuation on the output torque of the motor is suppressed. The velocity loop is responsible for stabilizing gimbal in inertial space and ensuring disturbance suppression performance.

The PWM power amplification component in Figure 3 is a proportional element. The velocity open-loop transfer function which is

$$\begin{aligned} P &= \frac{\omega_a}{I_r} \\ &= \frac{1}{JRs^2 + (JL + C_iK_iJ + f_mR)s + f_mL + C_mK_b + C_iK_if_m} \end{aligned} \tag{14}$$

The current closed-loop bandwidth is above 100 Hz, and $\frac{I_a}{I_r}$ is approximately be 1. Therefore, P can be further

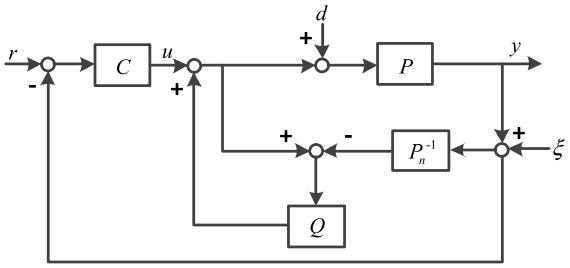

FIGURE 4. The standard DOB-based closed-loop system.

simplified to

$$P = \frac{\omega_a}{I_r} = \frac{C_i K_i C_m}{JRs^2 + (JL + C_i K_i J)s + C_m K_b + C_i K_i f_m} \tag{15}$$

In order to further improve the disturbance suppression performance of the gimbal system. A DOBC is introduced into feedback control loop in this paper. However, due to the nonlinear friction model and coupling, the velocity object characteristics of the gimbal will be subject to uncertainty perturbation. Even when the gimbal rotates clockwise and counterclockwise, the viscous friction coefficient f_m is different, and the direction of maximum static friction and coulomb friction are also different. Therefore, the traditional DOBC algorithm based on the model will have some observation errors, which is difficult to guarantee the robust stability of the system. For this problem, using an effective robust DOBC integrated design strategy to solve this problem is proposed in the next section.

III. ROBUST DOBC DESIGN

The essence of the DOBC is that, by the error between the given nominal model and the actual platform model, the errors are treated as a disturbance and fed forward to the forward channel in the closed-loop, ultimately achieving the elimination of system disturbances, as shown in Figure 4.

Multiplicative perturbation form of actual plant P is indicated by $P = (1+\Delta)P_n$, $\|\Delta\|_\infty \leq 1$. From the typical DOBC diagram in Figure 5, the relationship between the input u, noise ξ and output y of the DOBC can be obtained.

$$\begin{aligned} y = &\frac{P_n(1+\Delta)P_n}{P_n + ((1+\Delta)P_n - P_n)Q}u \\ &- \frac{(1+\Delta)P_nQ}{P_n + ((1+\Delta)P_n - P_n)Q}\xi \\ &- \frac{P_n(1+\Delta)P_n(1-Q)}{P_n + ((1+\Delta)P_n - P_n)Q}d \end{aligned} \tag{16}$$

Further it can be reduced to

$$y = \frac{(1+\Delta)P_n}{1+\Delta Q}u - \frac{(1+\Delta)Q}{1+\Delta Q}\xi - \frac{(1+\Delta)P_n(1-Q)}{1+\Delta Q}d \tag{17}$$

In practice, the effects of various disturbances and frictions are significant in the low-frequency range, while the influence of noise for system is significant in the high-frequency range.

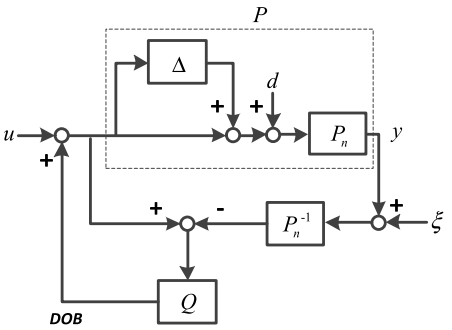

FIGURE 5. The typical DOB structure.

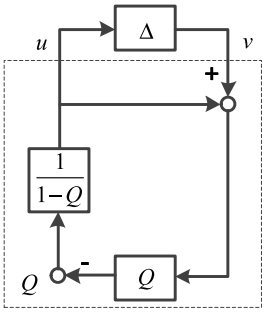

FIGURE 6. The general DOBC loop in the case of model uncertainty.

At the low-frequency, Δ is the upper bound of the uncertain change of the system model. When Q is approximately 1, it can suppress the influence of uncertainty Δ on the model output and eliminate the influence of disturbance d. At the high-frequency, due to the limitation of the closed-loop bandwidth, Δ can be neglected to be approximately 0. Q should tend to 0 and have strong signal attenuation capability in order to suppress noise effects. In summary, the design of the Q filter should be in the form of a low-pass filter. Only in this way can the suppression of low-frequency disturbances, uncertainties, and high-frequency noises be guaranteed simultaneously.

A. SENSITIVITY ANALYSIS

$1 - Q$ is regarded as the sensitivity function S of DOBC, and the corresponding complementary sensitivity function is $T = 1 - S = Q$. Thus, Figure 5 can be replaced by Figure 6.

The transfer function of u to v is Q in Figure 6. According to small-gain theory, the necessary conditions for DOBC to satisfy robust stability are:

$$\left\| W_T Q^{-1} \right\|_\infty < 1 \tag{18}$$

where W_T is an upper bound function of uncertainty Δ.

From Figure 5, we know that the sensitivity and complementary sensitivity function of the DOBC is equivalent to the transfer function of the input u to the output y. Therefore, the following form is derived as follows.

$$S_{DOB} = \frac{1-Q}{1+\Delta Q} \tag{19}$$

$$T_{DOB} = \frac{(1+\Delta)Q}{1+\Delta Q} \tag{20}$$

Assuming that $\Delta = 0$ for simplification, (17) is changed to

$$y = P_n u - Q\xi - P_n(1-Q)d \tag{21}$$

Considering that the requirements for low-frequency disturbance and uncertainty suppression performance conflict with the high-frequency noise suppression capability, it is necessary to design a suitable Q filter cutoff frequency to balance the performance of the system in the full-frequency band. Then $S_{DOB} = 1 - Q$, $T_{DOB} = Q$.The cost function of DOBC is defined by $H\infty$ norm.

$$\min_{\text{Q } stabilizaing} \left\| \begin{matrix} W_C(1-Q) \\ W_Q Q \end{matrix} \right\|_\infty \tag{22}$$

where the weight function W_C represents low-frequency suppression performance. its inverse represents the desired sensitivity at low frequencies, limiting the desired disturbance and the upper-bound of the uncertainty model. Similarly, noise suppression performance is expressed by the inverse of W_Q. However, equation (22) is not a standard robust $H\infty$ norm optimization problem, which is difficult to solve by DGKF algorithm.

B. Q FILTER SOLUTION

The general standard robust solution problem can be simply described which in a standard closed-loop feedback system defining the $H\infty$-norm optimization equation based on the performance weight function of the closed-loop system and solving the corresponding closed-loop controller C. When there is no DOBC in the closed-loop, the specific expression is as follows

$$\min_{C \ stabilizaing} \left\| \begin{matrix} W_P \dfrac{1}{1+PC} \\ W_M \dfrac{PC}{1+PC} \end{matrix} \right\|_\infty \tag{23}$$

where $\frac{1}{1+PC}$ and $\frac{PC}{1+PC}$ are the sensitivity and complementary function of closed-loop system without DOBC, W_P and W_M can be obtained by system design experiences and experimental testing.

When DOBC is introduced into inner loop of the closed-loop system, S_{clo} and T_{clo} can be respectively expressed by

$$S_{clo} = \frac{1-Q}{1+P_nC} = \frac{S_{DOB}}{1+P_nC} \tag{24}$$

$$T_{clo} = \frac{P_nC+Q}{1+P_nC} = \frac{P_nC+T_{DOB}}{1+P_nC} \tag{25}$$

Here S_{clo} and T_{clo} both no longer satisfy the preset conditions for solving the standard robust stability problem, and it is difficult to directly calculate the Q filter that realizes the expected performance. Three important issues need to be addressed in the process of transforming $H\infty$-based DOBC problems into a standard robust framework problem.

1. How to convert the problem into a standard robust solution problem;
2. How to ensure the robust stability of Q filter to the closed-loop system;
3. How to determine the weight function of Q filter.

For the first question, we define a scalar pseudo open-loop function $L = \tilde{P}K$, and $L = Q(1-Q)^{-1}$. Then Q and $1-Q$ can be expressed as $Q = L(1+L)^{-1}$ and $1-Q = (1+L)^{-1}$, respectively. After such the transformation, the relevant the cost function of DOBC is converted into a standard robust solution form. Where K is the robust controller solved by the DGKF solver. Therefore, the new cost function of DOBC is

$$\min_{\text{K } stabilizaing} \left\| \begin{matrix} W_C(1+\tilde{P}K)^{-1} \\ W_Q\tilde{P}K(1+\tilde{P}K)^{-1} \end{matrix} \right\|_\infty \tag{26}$$

According to given Theorem 1 in [22], the optimized loop function L is independent of the choice of $\tilde{P}$ and is uniquely determined when $\tilde{P}$ does not have any unstable poles and zeros except infinite zeros. Therefore, the selected $\tilde{P}$ will not have any effect on the norm minimization of the problem as long as it meets the requirements. When K is solved, the corresponding Q filter is also obtained.

The second and third question is considered simultaneously. In practice, it is not easy to directly give the performance weight function of Q filter. Therefore, we believe that the robust stability of designed Q filters based on robust stability boundary conditions W_P and W_M of the closed-loop system can be guaranteed when $\min_{Cstabilizaing} \left\| \begin{matrix} W_P S_{clo} \\ W_M T_{clo} \end{matrix} \right\|_\infty$ satisfies the robust stability requirement.

Therefore, the error cost function is rewritten by

$$\left\| W_P \frac{1-Q}{1+L} \right\|_\infty < 1 \tag{27}$$

Suppose the following (28) always exists

$$\left\| W_P \frac{1}{1+L} \right\|_\infty < W_{PD} \tag{28}$$

Then

$$\|W_{PD}(1-Q)\|_\infty < 1 \tag{29}$$

For robust stability of DOBC,

$$\|W_M T_{clo}\|_\infty < 1 \tag{30}$$

It can be converted into

$$\left\| W_M \frac{L+Q}{1+L} \right\|_\infty < 1 \tag{31}$$

$$|Q| < \left| W_M^{-1}(1+L) \right| - |L| \tag{32}$$

If W_{MD}^{-1} always satisfy (33)

$$|Q| < W_{MD}^{-1} < \left| W_M^{-1}(1+L) \right| - |L| \tag{33}$$

The new cost function can be obtained as

$$\|W_{MD}Q\|_\infty < 1 \tag{34}$$

The weight function of the Q filter is determined based on (28) and (33), and the Q filter design problem of (22) is finally evolved into the robust design problem described in (35).

$$\min_{\text{Q } stabilizaing} \left\| \begin{matrix} W_{PD}(1-Q) \\ W_{MD}Q \end{matrix} \right\|_\infty \tag{35}$$

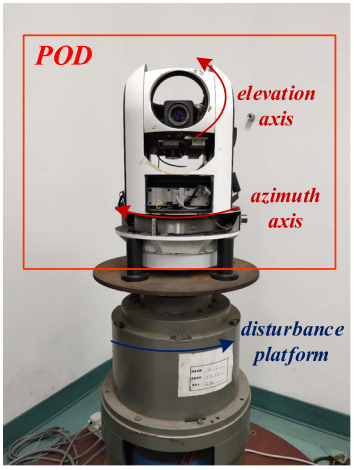

FIGURE 7. The pod experiment platform.

where W_{PD} is a redefined of W_C, W_{MD} is a redefined of W_Q. Therefore, (26) is redesigned as

$$\min_{\text{K } stabilizaing} \left\| \begin{matrix} W_{PD}(1+\tilde{P}K)^{-1} \\ W_{MD}\tilde{P}K(1+\tilde{P}K)^{-1} \end{matrix} \right\|_{\infty} \tag{36}$$

Finally, the final Q filter expression can be obtained by solving K with the hinfsyn function in the Matlab toolbox.

IV. EXPERIMENT VERFICATION

In the actual experimental, we use the two-axes pod system as the experimental platform for the robust DOBC control algorithm verification. The experimental platform is placed on a disturbance platform that can be rotated in azimuth to simulate external disturbances. Gyro sensors for measuring the velocity signal is mounted on the two rotating shafts of the pod and the disturbance platform. The electrical system of the entire experimental platform was implemented using a PC104-based control processing board. The system's interrupt execution frequency and sampling frequency are 1KHz. For the power drive unit module, a PI control algorithm is used to implement a current closed-loop bandwidth of above 120 Hz in the analog circuit board. The experimental platform is shown in Figure 7.

When the two axes of the gimbal are completely perpendicular to each other, the coupling torque is zero. Since the actual system inevitably has certain mechanical assembly errors, we have performed coupling measurements on two axes of the experimental platform. The experimental results are shown in Figure 8 and Figure 9. It can be seen that the coupling torque of the two axes is less than -25 dB within 30 Hz, and the influence of the coupling torque can be neglected. For coupling torques above 30 Hz, the influence of the coupling torque can also be approximately ignored because it is not within the velocity closed-loop operating bandwidth of the system (<30 Hz). Ignoring the influence of coupling torque, the other characteristics of the two axes are consistent. Therefore, the azimuth-axis is selected as the control object in the experiment.

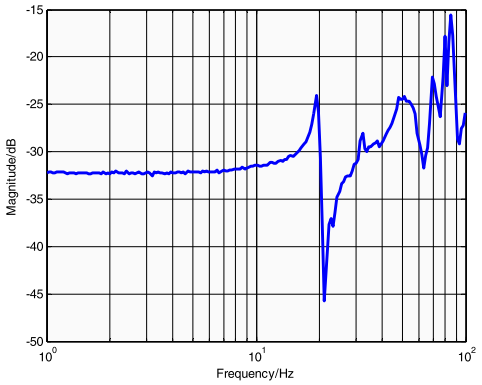

FIGURE 8. The cross-coupling result of azimuth-axis.

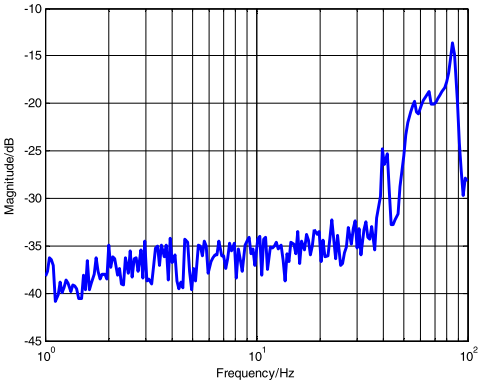

FIGURE 9. The cross-coupling result of elevation-axis.

The velocity open-loop characteristic G_v of the azimuth rotation axis of the pod is composed of two one-order low-pass filters.

$$G_v = \frac{2.2}{(0.075s+1)(0.001s+1)}$$

The corresponding velocity controller C_v is designed as

$$C_v = 550\frac{(0.24s+1)(0.046s+1)}{(1.6s+1)(1.3s+1)}$$

The designed open-loop characteristic is 10.2dB amplitude margin, 54.3deg phase margin, and open-loop cut-off frequency of 14.3Hz. Ultimately, a 20Hz velocity closed-loop bandwidth is achieved. According to the suppression performance and closed-loop response of the closed-loop system, $W_P = \frac{3.333s+65}{s+0.65}$ and $W_M = \frac{0.008s+1}{2}$ are selected as the performance constraint weight functions of the closed-loop system, as shown in Figure 10 and Figure 11. The DOBC design based on the weight function can guarantee the robustness of both the closed-loop system and the DOBC itself.

$\tilde{P}$ is set to a second-order low-pass form, and the cutoff frequency of L is consistent with the open-loop cutoff frequency after velocity closed-loop achieved. The open-loop characteristic after the actual closed-loop system is shown in Figure 12. L is approximately $\frac{50}{0.5s+1}$. According to equations (28)

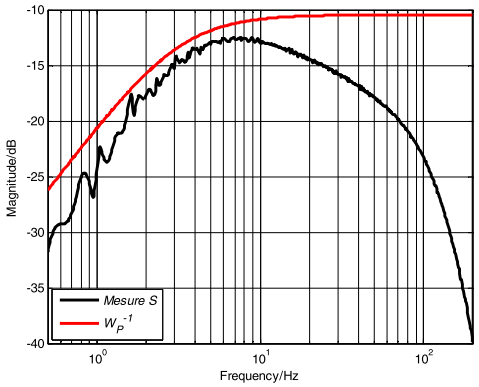

FIGURE 10. The sensitivity function design of closed-loop system.

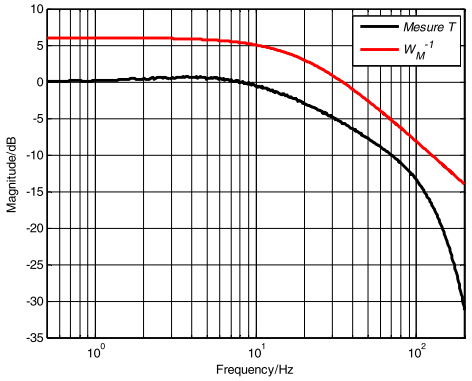

FIGURE 11. The complementary sensitivity function design of closed-loop system.

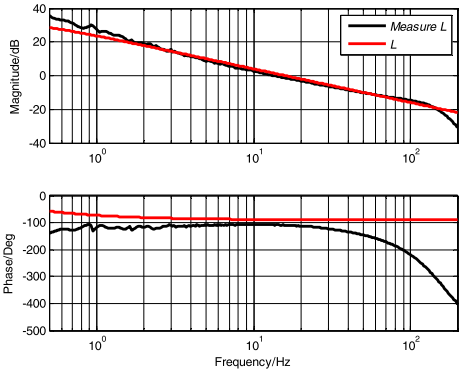

FIGURE 12. The open-loop characteristic of closed-loop system.

and (33), the constraint weight functions of the DOBC are further obtained as follows:

$$\tilde{P} = \frac{1}{0.0001s^2 + 0.004s + 1}$$
$$W_{PD} = 5\frac{s+60}{s+5}$$
$$W_{MD} = \frac{(0.05s+1)}{3.8}$$

Based on the function given above, substituting into the $H\infty$ formula solver of Matlab, the K controller and the final

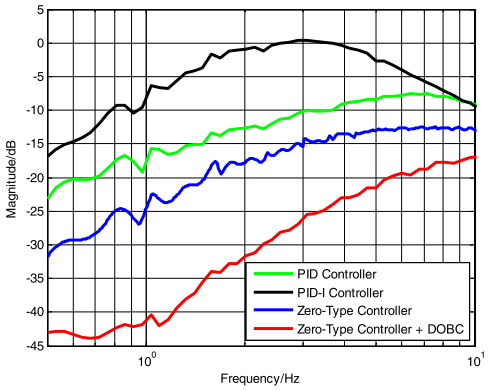

FIGURE 13. Comparative results of disturbance suppression characteristics in frequency domain.

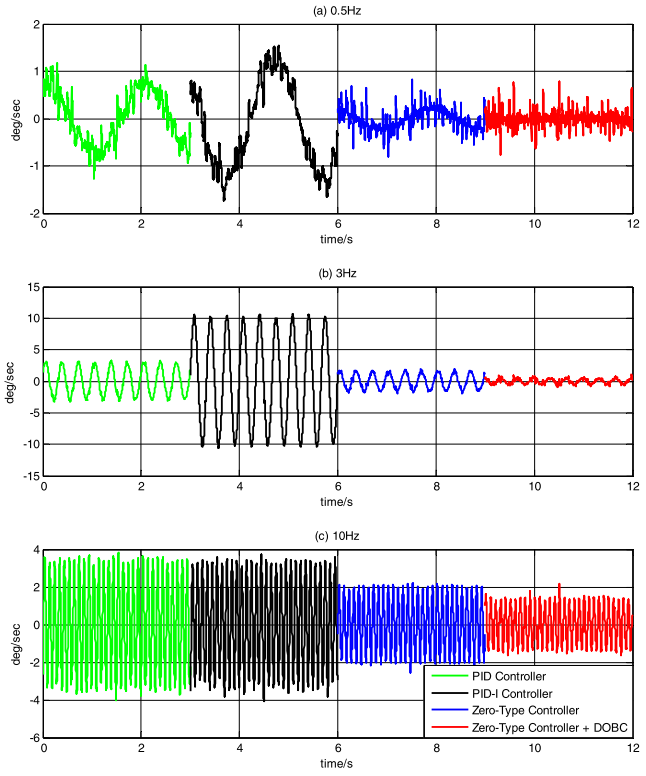

FIGURE 14. Comparison of disturbance suppression performance in time domain; (a) disturbance input frequency 0.5HZ; (b) disturbance input frequency 3HZ; (c) disturbance input frequency 10HZ.

Q filter are obtained.

$$K = \frac{1.658\text{e}04s + 4.045\text{e}06}{s^2 + 7.434\text{e}04s + 3.717\text{e}05}$$
$$Q = \frac{4.0451\text{e}06}{(s + 7.433\text{e}04)(s + 59.46)}$$

The ways to improve the disturbance suppression performance of control system are feedforward compensation and improving the open-loop gain of system. Improving the system type, that is, increasing the number of integral in the front channel of the system, is a common method to improve the low-frequency gain of the system. In order to prove the progressiveness of robust DOBC, four groups experiments

based on PID, PID-I, zero-type controller and zero-type plus DOBC were designed and implemented in this paper.

In the experiment, the disturbance platform produces a sinusoidal output signal with a 0.5 to 10 Hz amplitude of 10 deg/sec and a variable frequency. The reference input of pod system is 0. The measurement results of the disturbance suppression comparison shown in Figure 13 are obtained, and Figure 14 shows the azimuth-axis output of the pod system on the disturbance input frequency of 0.5 Hz, 3 Hz, and 10 Hz. Through experiments, it can be analyzed that although PID and PID-I can improve the system type, the phase attenuation of the system is severe due to the integral, which reduces the low-frequency open-loop gain in order to satisfy the stability margin of the system. Therefore, the design method of the zero-type controller is more advantageous for two-axes gimbal system. Realizing robust DOBC based on the zero-type controller can further improve the disturbance suppression performance of the system. Especially, the suppression performance at 0.5 Hz is improved by about −11 dB with respect to the zero-type controller.

V. CONCLUSION

Aiming at the disturbance suppression problem faced by the two-axes gimbal systems, this paper proposes a robust DOBC-based disturbance compensation method. Friction, coupling and external disturbances affecting the performance of the gimbal system are compensated by the DOBC feedforward loop. Because nonlinear friction can result in uncertainty problem, a low-pass filter design scheme for DOBC under the standard $H\infty$ problem framework is further designed. The weight function of the DOBC in this scheme is determined based on the sensitivity function and the complementary sensitivity function of the actual closed-loop system, thus ensuring the robustness of the DOBC to the closed-loop system. The experiment results demonstrate good disturbance suppression ability and robust performance of the proposed robust DOBC design method. However, final disturbance compensation performance of the robust design of DOBC, in order to ensure its own and the robustness to the system, may be conservative. Therefore, the future research work will attempt to establish some nonlinear estimation models in the DOBC's nominal model to further improve the disturbance suppression capability.

REFERENCES

[1] M. K. Masten, "Inertially stabilized platforms for optical imaging systems," *IEEE Control Syst.*, vol. 28, no. 1, pp. 47–64, Feb. 2008.

[2] R. Fields, D. Kozlowski, H. Yura, R. Wong, J. Wicker, C. Lunde, M. Gregory, B Wandernoth, and F. Heine, "5.625 Gbps bidirectional laser communications measurements between the NFIRE satellite and an optical ground station," in *Proc. Int. Conf. Space Opt. Syst. Appl. (ICSOS)*, May 2011, pp. 44–53.

[3] B. L. Ulich, "Overview of acquisition, tracking, and pointing system technologies," *Proc. SPIE*, vol. 0887, no. 24, pp. 40–63, May 1988.

[4] J. M. Hilkert and D. L. Amil, "Structural effects and techniques in precision pointing and tracking systems: A tutorial overview," *Proc. SPIE*, vol. 7696, May 2010, Art. no. 76961C.

[5] J. M. Hilkert, "Inertially stabilized platform technology concepts and principles," *IEEE Control Syst. Mag.*, vol. 28, no. 1, pp. 26–46, Feb. 2008.

[6] J. Krishnamoorty, R. Marathe, and V. Sule, "H∞ control law for line-of-sight stabilization for mobile land vehicles," *Proc. SPIE*, vol. 41, no. 11, pp. 2935–2945, Nov. 2002.

[7] S. B. Kim, S. H. Kim, and Y. K. Kwak, "Robust control for a two-axis gimbaled sensor system with multivariable feedback systems," *IET Control Theory Appl.*, vol. 4, no. 4, pp. 539–551, 2010.

[8] M. Baskin and M. K. Leblebicioğlu, "Robust control for line-of-sight stabilization of a two-axis gimbal system," *Turkish J. Electr. Eng. Comput. Sci.*, vol. 25, no. 5, pp. 3839–3853, Oct. 2017.

[9] B. Li, D. Hullender, and M. DiRenzo, "Nonlinear induced disturbance rejection in inertial stabilization systems," *IEEE Trans. Control Syst. Technol.*, vol. 6, no. 3, pp. 421–427, May 1998.

[10] P. Cui, D. Zhang, S. Yang, and H. Li, "Friction compensation based on time-delay control and internal model control for a gimbal system in magnetically suspended CMG," *IEEE Trans. Ind. Electron.*, vol. 64, no. 5, pp. 3798–3807, May 2017.

[11] B. Ahi and A. Nobakhti, "Hardware implementation of an ADRC controller on a gimbal mechanism," *IEEE Trans. Control Syst. Technol.*, vol. 26, no. 6, pp. 2268–2275, Nov. 2018.

[12] M. M. Abdo, A. R. Vali, A. R. Toloei, and M. R. Arvan, "Stabilization loop of a two axes gimbal system using self-tuning PID type fuzzy controller," *ISA Trans.*, vol. 53, no. 2, pp. 591–602, Mar. 2014.

[13] A. Naderolasli and M. Tabatabaei, "Stabilization of the two-axis gimbal system based on an adaptive fractional-order sliding-mode controller," *IETE J. Res.*, vol. 63, no. 1, pp. 124–133, 2017.

[14] K. Ohnishi, "A new servo method in mechatronics," *Trans. Jpn. Soc. Electr. Eng. D*, vol. 177, pp. 83–86, 1987.

[15] K. S. Eom, I. H. Suh, and W. K. Chung, "Disturbance observer based path tracking control of robot manipulator considering torque saturation," *Mechatronics*, vol. 11, no. 3, pp. 325–343, Apr. 2001.

[16] H. Shim and N. H. Jo, "An almost necessary and sufficient condition for robust stability of closed-loop systems with disturbance observer," *Automatica*, vol. 45, no. 1, pp. 296–299, Jan. 2009.

[17] W. Xie, "High frequency measurement noise rejection based on disturbance observer," *J. Franklin Inst.*, vol. 347, no. 10, pp. 1825–1836, Dec. 2010.

[18] N. H. Jo, C. Jeon, and H. Shim, "Noise reduction disturbance observer for disturbance attenuation and noise suppression," *IEEE Trans. Ind. Electron.*, vol. 64, no. 2, pp. 1381–1391, Feb. 2017.

[19] Y. Choi, K. Yang, W. K. Chung, H. R. Kim, and I. H. Suh, "On the robustness and performance of disturbance observers for second-order systems," *IEEE Trans. Autom. Control*, vol. 48, no. 2, pp. 315–320, Feb. 2003.

[20] A. Tesfaye, H. S. Lee, and M. Tomizuka, "A sensitivity optimization approach to design of a disturbance observer in digital motion control systems," *IEEE/ASME Trans. Mechatronics*, vol. 5, no. 1, pp. 32–38, Mar. 2000.

[21] J. R. Ryoo, T.-Y. Doh, and M. J. Chung, "Robust disturbance observer for the track-following control system of an optical disk drive," *Control Eng. Pract.*, vol. 12, no. 5, pp. 577–585, May 2004.

[22] J. Su, L. Wang, and J. Yun, "A design of disturbance observer in standard H∞ control framework," *Int. J. Robust Nonlinear Control*, vol. 25, no. 16, pp. 2894–2910, Nov. 2015.

[23] C.-C. Wang and M. Tomizuka, "Design of robustly stable disturbance observers based on closed loop consideration using H/sub /spl infin// optimization and its applications to motion control systems," in *Proc. Amer. Control Conf.*, Jun./Jul. 2004, pp. 3764–3769.

[24] T. Mita, M. Hirata, K. Murata, and H. Zhang, "H/sub /spl infin// control versus disturbance- observer-based control," *IEEE Trans. Ind. Electron.*, vol. 45, no. 3, pp. 488–495, Jun. 1998.

WEI REN was born in Nanchong, China, in 1993. He received the M.S. degree from the Institute of Optics and Electronics, Chinese Academy of Sciences, in 2017, where he is currently pursuing the Ph.D. degree in optoelectronic engineering.

He is with the Key Laboratory of Beam Control, the Institute of Optics and Electronics, Chinese Academy of Sciences. His research interests include optical signal processing, electro-optical tracking control, and intelligent control.

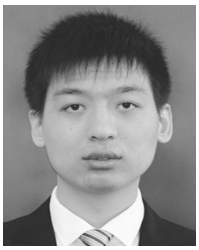

QI QIAO was born in Shanxi, China, in 1994. He received the B.S. degree in automation from Southwest University, in 2017. He is currently pursuing the M.S. degree with the Institute of Optics and Electronics, Chinese Academy of Sciences.

His research interests include PCB design and ARM embedded systems. His current research interest includes sliding model control in the electro-optical tracking systems.

KANG NIE was born in Nanchang, China, in 1995. He received the B.S. degree in automation from Southwest University, in 2017. He is currently pursuing the M.S. degree in signal processing with the Institute of Optics and Electronics, Chinese Academy of Sciences, where he is with the Key Laboratory of Beam Control.

His research interests include electro-optical tracking control, active disturbance rejection control, and intelligent control.

YAO MAO received the B.S. degree from Chongqing University and the Ph.D. degree in signal processing from the Institute of Optics and Electronics, Chinese Academy of Sciences, in 2001 and 2012, respectively, where he is currently a Professor and the Doctor Director.

His research interests include servo control, predictive filtering, and machine learning.